



Figures and figure supplements

Mechanistic insights into a TIMP3-sensitive pathway constitutively engaged in the regulation of cerebral hemodynamics

Carmen Capone *et al*

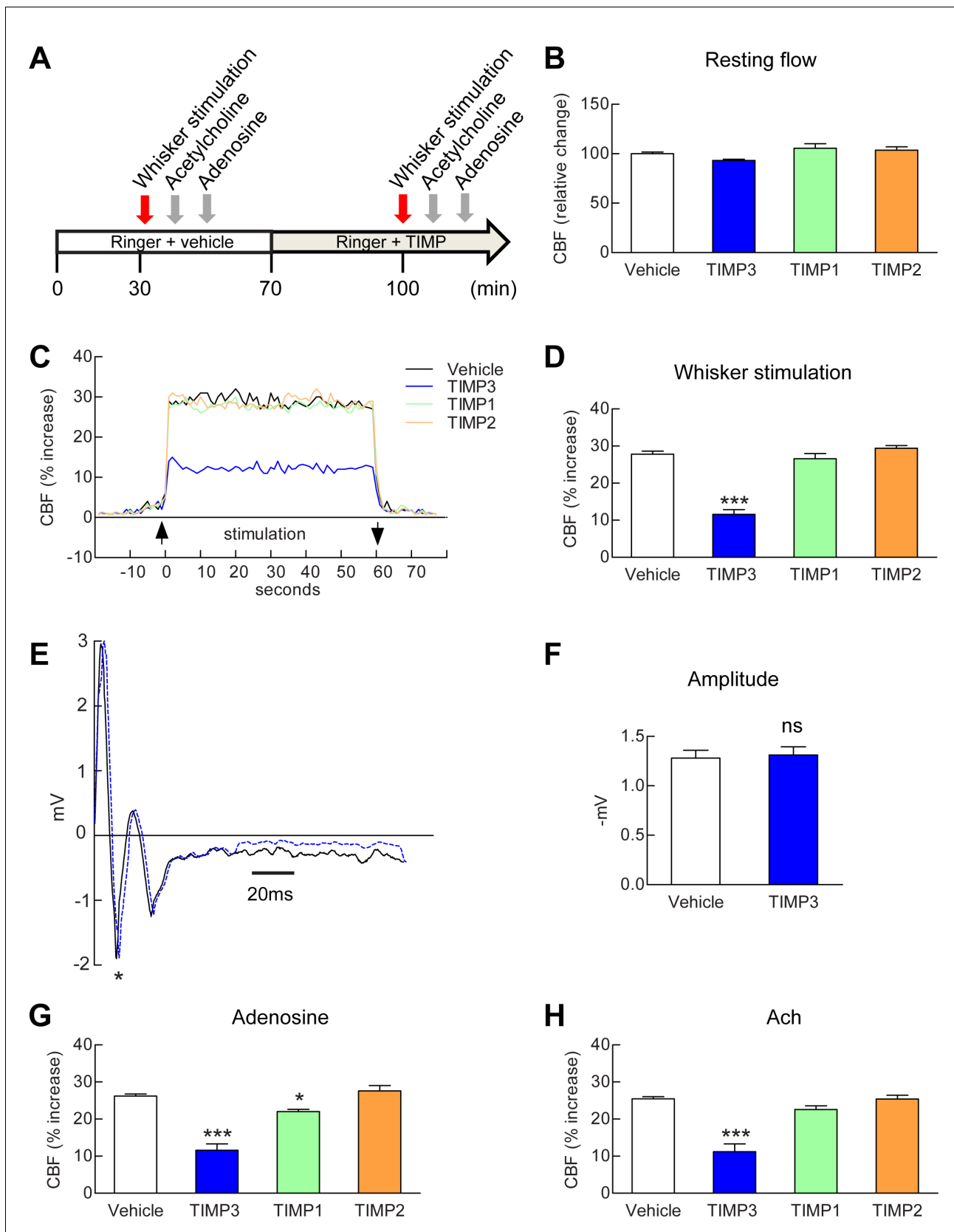


Figure 1. Exogenous TIMP3 specifically impairs cerebrovascular reactivity. (A) Schematic representation of the experimental protocol used to test the effects of recombinant TIMP1 (50 nM), TIMP2 (50 nM) or TIMP3 (40 nM) superfusion on the somatosensory cortex of 2-month-old wild-type mice. (B–D) Figure 1 continued on next page

Figure 1 continued

Resting CBF (B) and CBF responses to whisker stimulation (C, D) were evaluated upon superfusion of vehicle or TIMP proteins. (C) Representative trace of CBF responses to whisker stimulation upon superfusion of vehicle or TIMP proteins (C). (E) Representative trace of the field potentials evoked by whisker stimulation upon vehicle or TIMP3 superfusion, showing typical sharp positive (P1)-negative (N1) waves followed by a slower positive-negative waveform occurring within 80 ms post stimulus (Di and Barth, 1991). (F) The amplitude of the negative wave (N1, asterisk in E) of the field potential was not affected by TIMP3 superfusion ($p=0.79$). (G, H) CBF responses to topical application of adenosine (G) or acetylcholine (H) upon superfusion of vehicle or TIMP proteins. Significance was determined by one-way ANOVA followed by Tukey's post-hoc test (B, D, G, H) or unpaired Student's t-test (F). (* $p<0.05$, *** $p<0.001$ compared to vehicle; $n = 5$ mice/groups). Error bars indicate SEM.

DOI: [10.7554/eLife.17536.003](https://doi.org/10.7554/eLife.17536.003)

The following source data is available for figure 1:

Source data 1. Reagents used for **Figure 1**.

DOI: [10.7554/eLife.17536.004](https://doi.org/10.7554/eLife.17536.004)

Source data 2. Main physiological variables of mice studied in **Figure 1**.

DOI: [10.7554/eLife.17536.005](https://doi.org/10.7554/eLife.17536.005)

Source data 3. Numerical data that were used to generate the bar charts in **Figure 1**.

DOI: [10.7554/eLife.17536.006](https://doi.org/10.7554/eLife.17536.006)

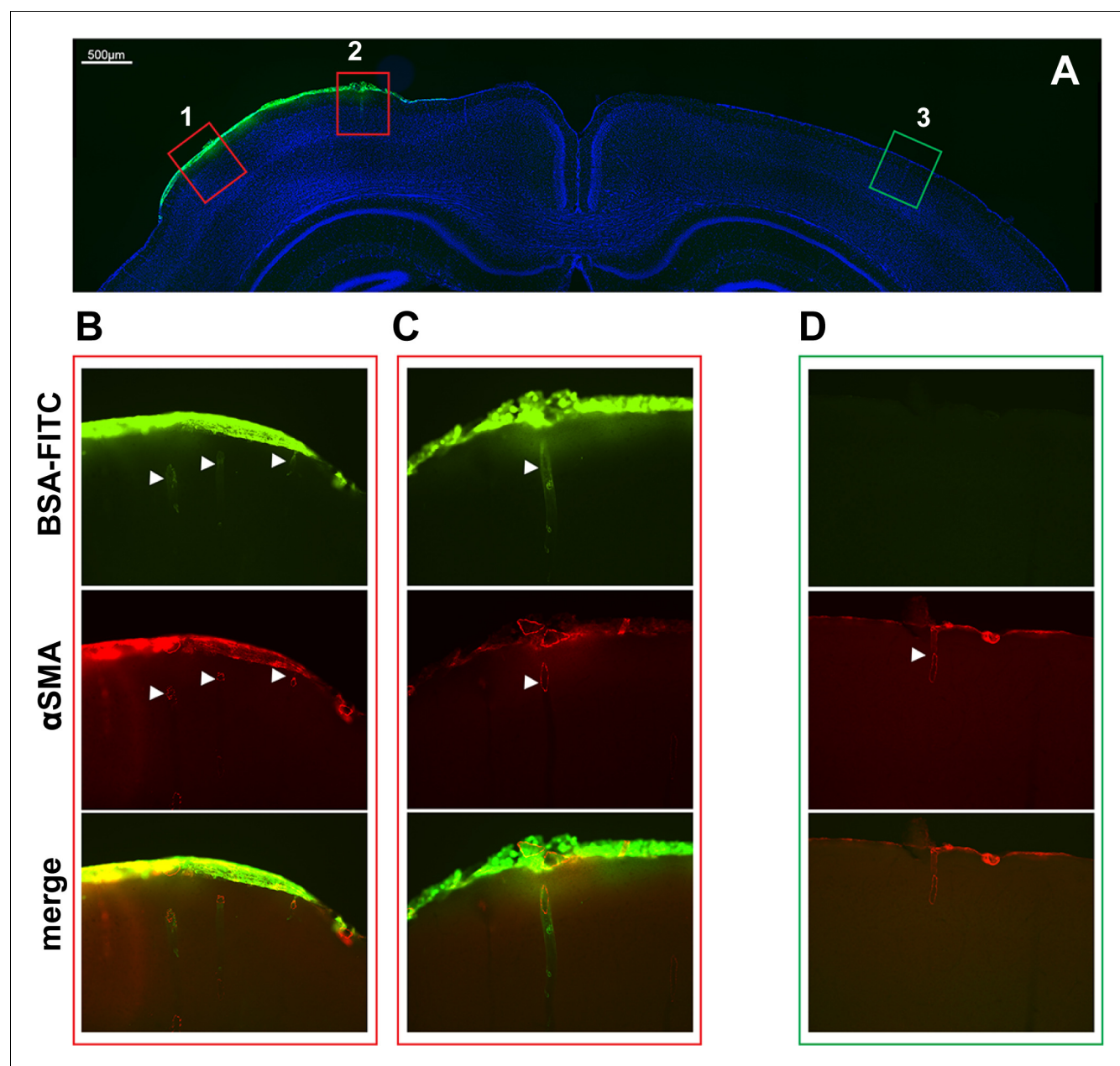


Figure 1—figure supplement 1. Assessment of brain penetration of fluorescein isothiocyanate labelled serum albumin (FITC-BSA) superfused over the cranial window. (A) FITC-BSA was topically superfused over the somatosensory cortex for 30 min, the brain was removed at the time of killing, post-fixed, sectioned in 50- μ m-thick coronal slices through the perfusion site using a vibratome and immunostained with anti-smooth muscle alpha actin conjugated to Alexa 594 (α -SMA). Shown is a representative vibratome coronal section counterstained with DAPI and examined by epifluorescence microscopy (merge of DAPI and FITC images). The pia matter as well the penetrating vessels under the window (left side) display spontaneous FITC fluorescence. (B–D) Higher magnification of selected regions ipsilateral to the window (1-B, 2-C) or contralateral to the window (3-D), delineated in A, showing that FITC-BSA entered the cortex along the penetrating arteries (white arrowheads) beneath the cranial window (B, C). Scale bar represents 500 μ m (A) and 100 μ m (B–D).

DOI: [10.7554/eLife.17536.007](https://doi.org/10.7554/eLife.17536.007)

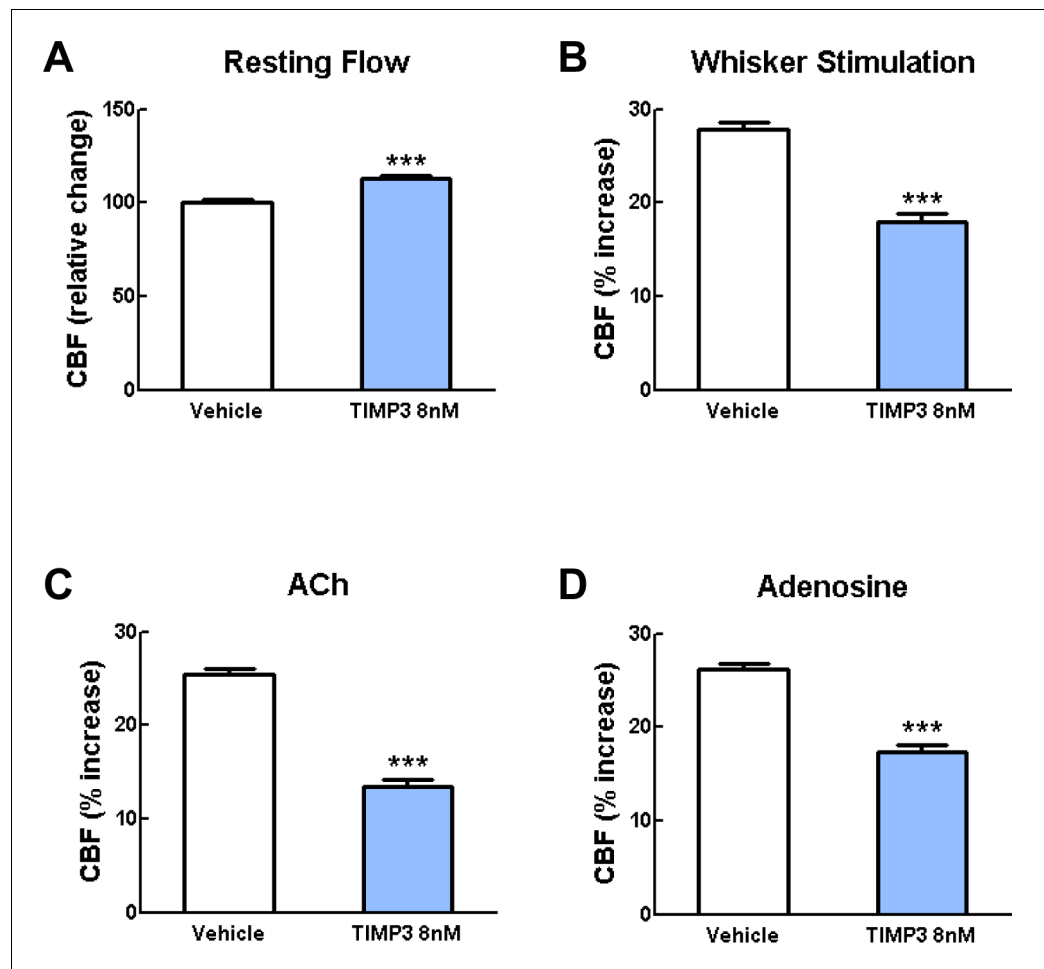


Figure 1—figure supplement 2. Exogenous TIMP3 (8 nM) impairs cerebrovascular reactivity. (A–D) Resting CBF (A) and CBF responses to whisker stimulation (B) or topical application of acetylcholine (C) or adenosine (D) were evaluated upon superfusion of TIMP3 (8 nM) or vehicle. Significance was determined by one-way ANOVA followed by Tukey's post-hoc test. (***) $p < 0.001$ compared with vehicle; $n = 5$ mice/group).

DOI: [10.7554/eLife.17536.008](https://doi.org/10.7554/eLife.17536.008)

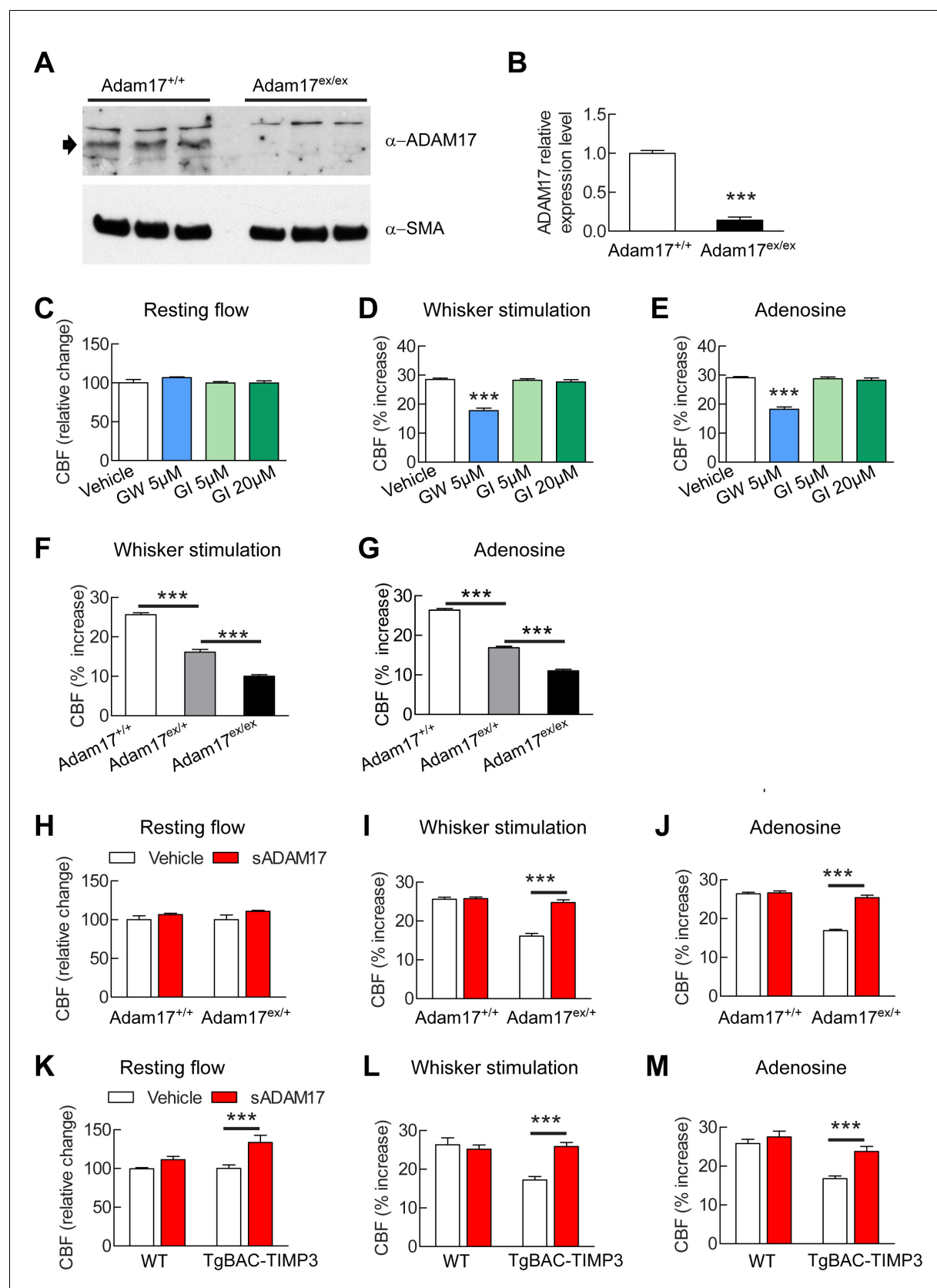


Figure 2. Cerebrovascular responses are impaired by pharmacological or genetic inhibition of ADAM17, and rescued by exogenous sADAM17. (A) Immunoblot of cerebral arteries dissected from *Adam17^{+/+}* and *Adam17^{ex/ex}* mice ($n = 3$ biological samples/genotype) incubated with anti-ADAM17 or Figure 2 continued on next page

Figure 2 continued

anti-smooth muscle α -actin (α -SMA) antibody. (B) Quantification of relative protein level of ADAM17 in (A). (C–E) Resting CBF (C) and CBF responses to whisker stimulation (D) or topical application of adenosine (E) were evaluated upon superfusion of the dual ADAM10/ADAM17 inhibitor GW413333X (GW; 5 μ M) or the ADAM10 inhibitor GI254023X (GI; 5 and 20 μ M). *** $p < 0.05$ compared with vehicle. (F, G) CBF responses to whisker stimulation (F) or topical application of adenosine (G) were strongly reduced in *Adam17^{ex/+}* mice and further reduced in *Adam17^{ex/ex}* mice compared with wild-type littermate controls. (H–J) Exogenous sADAM17 (16 nM) significantly ameliorated CBF responses to whisker stimulation (I) or topical application of adenosine (J) in *Adam17^{ex/+}* mice, whereas ADAM17 had no effect on wild-type littermates. (K–M) Resting CBF and CBF responses were evaluated in *TgBAC-TIMP3* mice and non-transgenic littermates (WT) before and after superfusion of ADAM17. CBF responses to whisker stimulation (L) or topical application of adenosine (M) were strongly reduced in *TgBAC-TIMP3* mice compared with those in WT mice, as previously reported (Capone et al., 2016), and were normalized by sADAM17 superfusion. Significance was determined by one-way ANOVA followed by Tukey's post-hoc test (B–G) and two-way repeated measure ANOVA followed by Bonferroni post-hoc test (H–M) ($n = 5$ mice/group). Error bars indicate SEM.

DOI: [10.7554/eLife.17536.009](https://doi.org/10.7554/eLife.17536.009)

The following source data is available for figure 2:

Source data 1. Reagents used for Figure 2.

DOI: [10.7554/eLife.17536.010](https://doi.org/10.7554/eLife.17536.010)

Source data 2. Main physiological variables of mice studied in Figure 2.

DOI: [10.7554/eLife.17536.011](https://doi.org/10.7554/eLife.17536.011)

Source data 3. Numerical data that were used to generate the bar charts in Figure 2.

DOI: [10.7554/eLife.17536.012](https://doi.org/10.7554/eLife.17536.012)

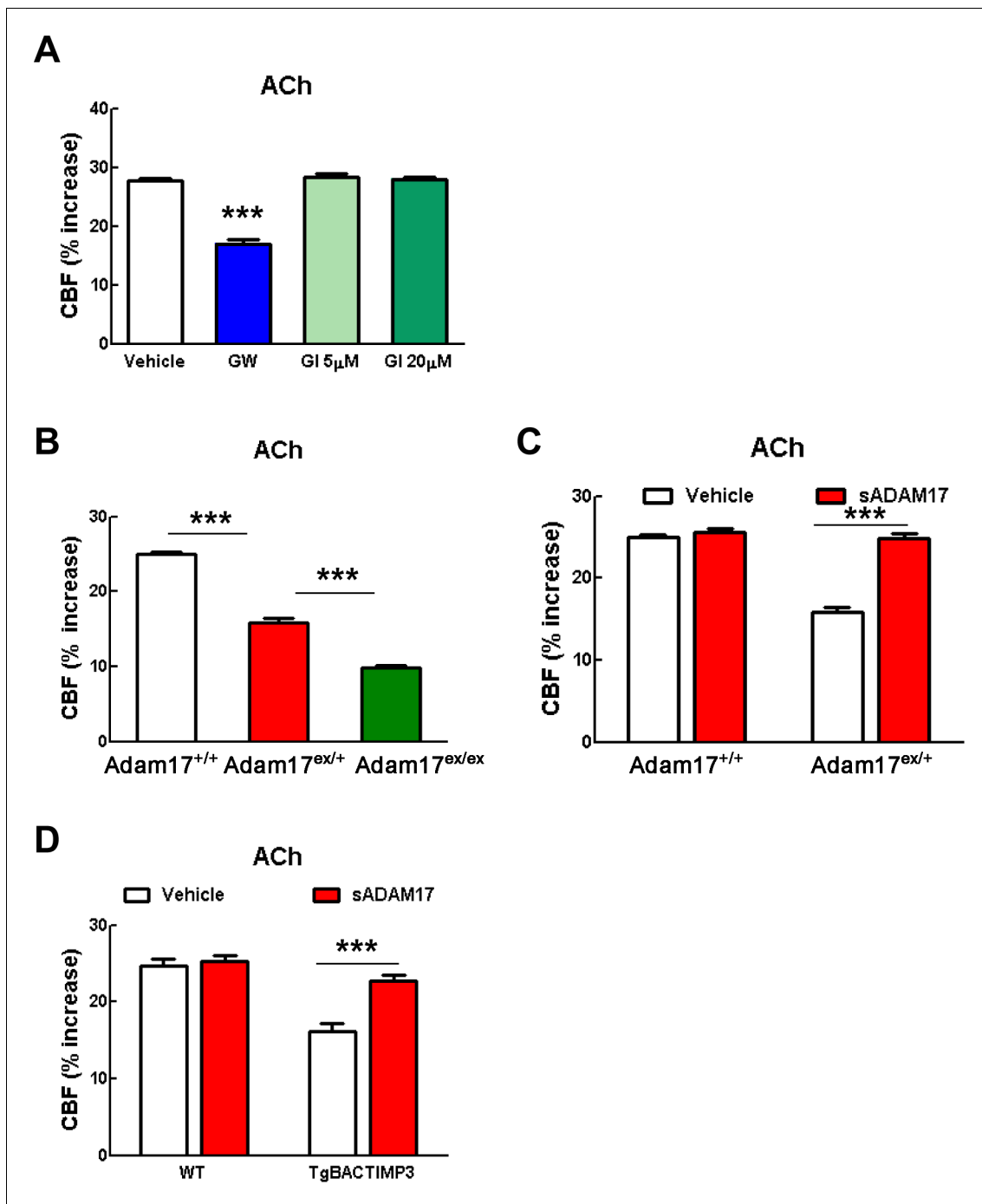


Figure 2—figure supplement 1. CBF responses to acetylcholine are attenuated by pharmacological or genetic inhibition of ADAM17 but rescued upon superfusion of exogenous sADAM17. (A) CBF responses to topical application of acetylcholine were evaluated in 2-month-old wild-type mice upon superfusion of the dual ADAM10/ADAM17 inhibitor GW413333X (GW; 5 μ M) or the ADAM10 inhibitor GI254023X (GI; 5 and 20 μ M). *** p <0.001 compared with vehicle. (B) CBF responses to topical application of acetylcholine were strongly reduced in Adam17^{ex/+} mice and further reduced in Adam17^{ex/ex} mice compared to littermate wildtype (WT) mice. (C) Exogenous soluble active ectodomain of ADAM17 (sADAM17; 16 nM) significantly ameliorated CBF responses to topical application of acetylcholine in Adam17^{ex/+} mice, whereas it had no effect on wild-type littermates. (D) CBF responses to topical application of acetylcholine were strongly reduced in TgBAC-TIMP3 mice compared with those in WT mice, as previously reported (Capone et al., 2016), and were normalized by sADAM17 superfusion. Significance was determined by one-way ANOVA followed by Tukey's post-hoc test (A, B) and two-way repeated measure ANOVA followed by Bonferroni post-hoc test (C, D) (n = 5 mice/group).

DOI: 10.7554/eLife.17536.013

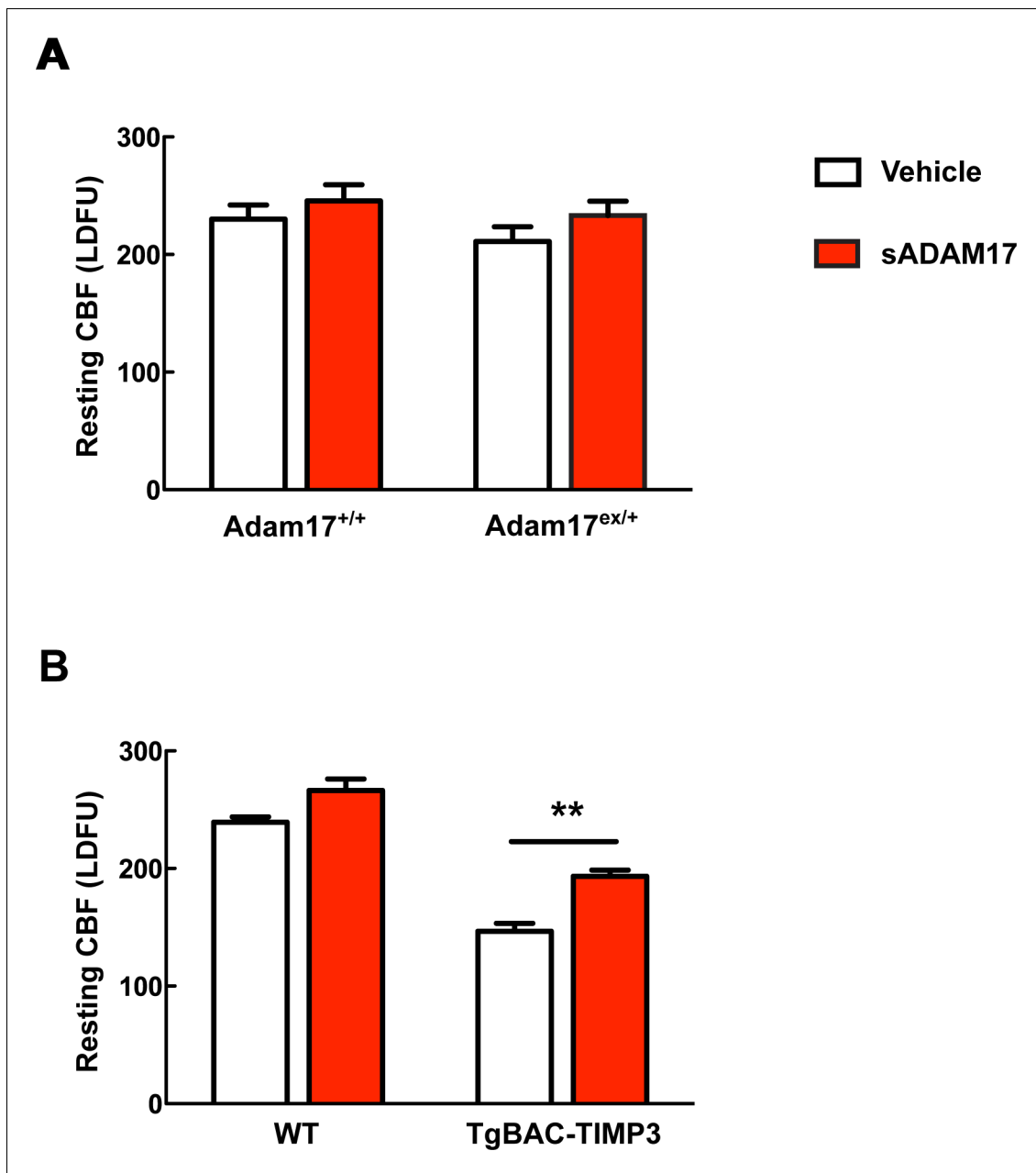


Figure 2—figure supplement 2. Absolute measurements of resting CBF in *Adam17^{ex/+}* and *TgBAC-TIMP3* mice in the presence and absence of sADAM17. Resting CBF, expressed as Laser Doppler flow arbitrary units (LDFU), was evaluated in *Adam17^{ex/+}* mice (A), *TgBAC-TIMP3* mice (B) and appropriate wild-type littermates, before and after superfusion of soluble ADAM17 (16 nM). Significance was determined by two-way repeated measures ANOVA followed by Bonferroni post-hoc test ($n = 5$ mice/group).

DOI: [10.7554/eLife.17536.014](https://doi.org/10.7554/eLife.17536.014)

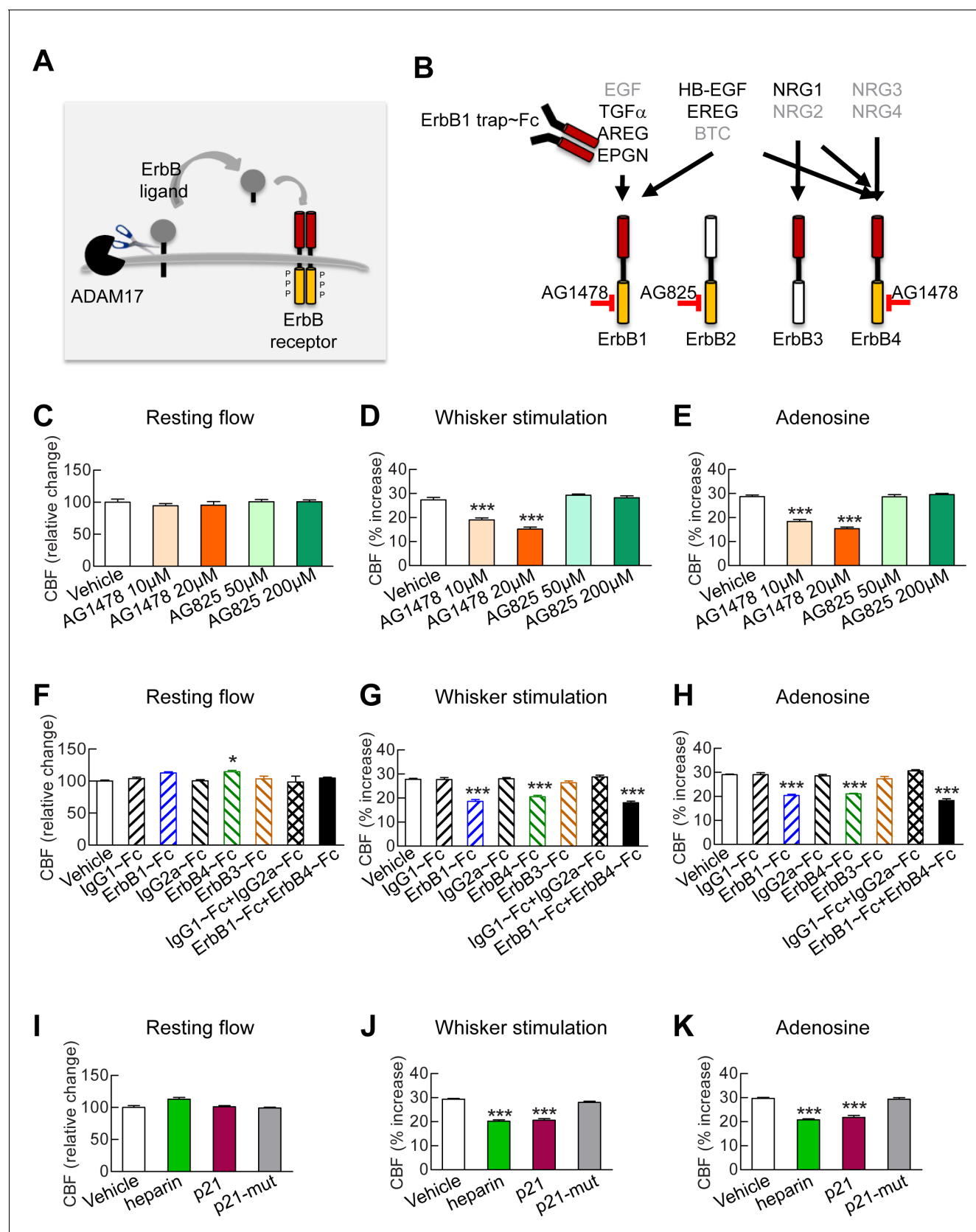


Figure 3. Full CBF responses require ErbB1/ErbB4 and HB-EGF. (A, B) Schematic representation of the ErbB signaling pathway. Ligands are all produced as membrane-bound precursor proteins that are cleaved by cell-surface sheddases to yield the active growth factor species. Binding of the

Figure 3 continued on next page

Figure 3 continued

soluble form of the ligand induces ErbB receptor homodimerization or heterodimerization, converting the receptor to an active dimeric conformation (A). Ligands are grouped in four rows according to their receptor specificity (top; arrows); the six ligands for which ectodomain shedding is primarily mediated by ADAM17 appear in black characters, and the remaining five are in grey characters (B). (C–K) Resting CBF (C, F, I) and CBF responses to whisker stimulation (D, G, J) or topical application of adenosine (E, H, K) were evaluated before and after superfusion of various inhibitors of the ErbB signaling pathway, including the ErbB1/ErbB4 inhibitor AG1478 (10 and 20 μ M); the ErbB2 inhibitor AG825 (50 and 200 μ M) (C–E), the soluble ErbB receptor traps (ErbB1-Fc, 66.7 nM; ErbB3-Fc, 71.4 nM; ErbB4-Fc, 71.4 nM) and the respective control IgG1-Fc and IgG2-Fc fragments (286 nM) (F–H), heparin and the synthetic peptide p21 (12 μ M) and the control inactive peptide p21-mut (12 μ M) (I–K). None of these compounds affected resting CBF, except ErbB4-Fc, which produced a slight increase. (C–K) Significance was determined by one-way ANOVA followed by Tukey's post-hoc test (* $p < 0.05$, ** $p < 0.01$, *** $p < 0.001$ compared to vehicle; $n = 5/\text{group}$). Error bars indicate SEM.

DOI: [10.7554/eLife.17536.015](https://doi.org/10.7554/eLife.17536.015)

The following source data is available for figure 3:

Source data 1. Reagents used for **Figure 3**.

DOI: [10.7554/eLife.17536.016](https://doi.org/10.7554/eLife.17536.016)

Source data 2. Main physiological variables of mice studied in **Figure 3**.

DOI: [10.7554/eLife.17536.017](https://doi.org/10.7554/eLife.17536.017)

Source data 3. Numerical data that were used to generate the bar charts in **Figure 3**.

DOI: [10.7554/eLife.17536.018](https://doi.org/10.7554/eLife.17536.018)

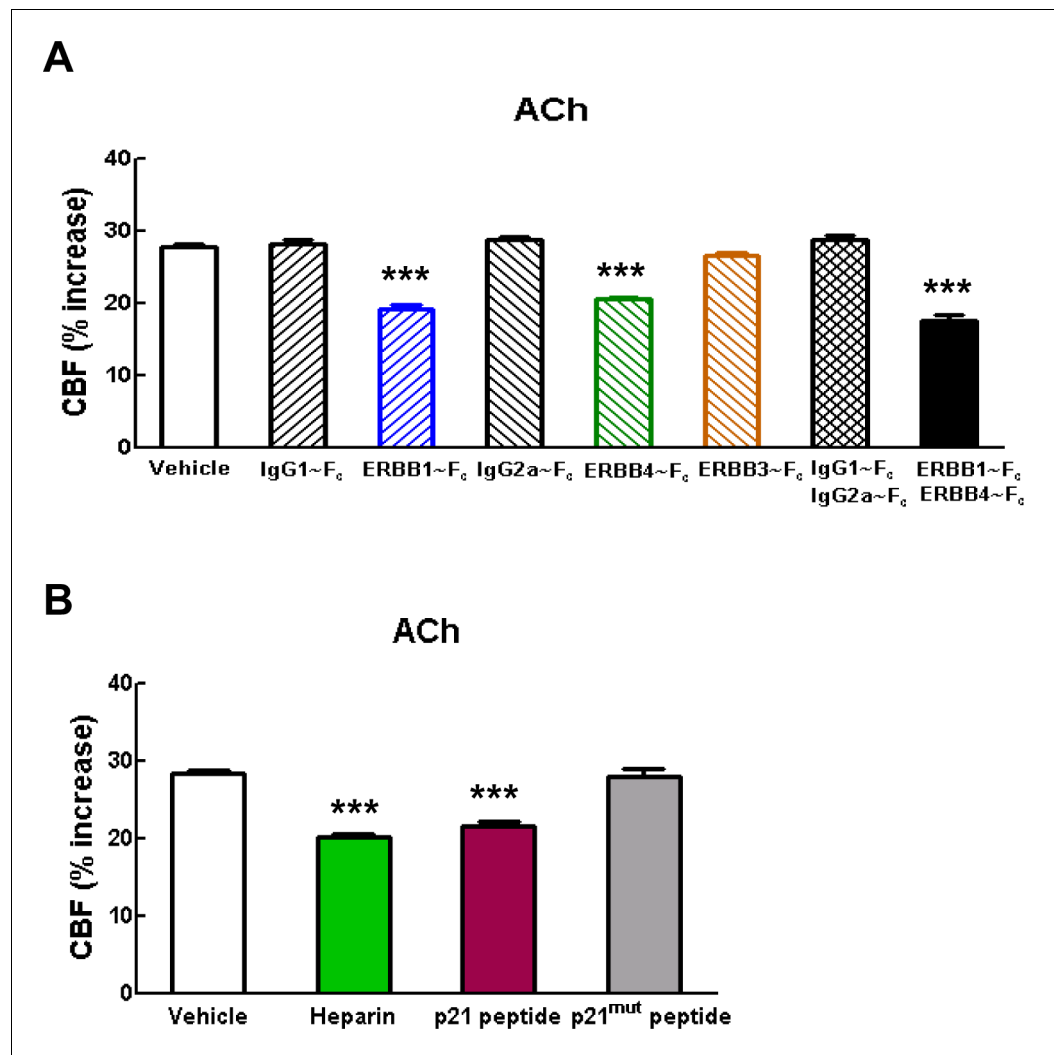


Figure 3—figure supplement 1. Blockade of ErbB1/ErbB4 or HB-EGF impairs CBF responses to acetylcholine. (A, B) CBF responses to application of acetylcholine were evaluated before and after superfusion of various inhibitors of the ErbB signaling pathway, including the soluble ErbB receptor traps (ErbB1-Fc, 66.7 nM; ErbB3-Fc, 71.4 nM; ErbB4-Fc, 71.4 nM) and the respective control IgG1-Fc and IgG2-Fc fragments (286 nM) (A), heparin and the synthetic peptide p21 (12 μ M) and the control inactive peptide p21-mut (12 μ M) (B). Significance was determined by one-way ANOVA followed by Tukey's post-hoc test. (***) $p < 0.001$ compared with vehicle; $n = 5$ /group).

DOI: [10.7554/eLife.17536.019](https://doi.org/10.7554/eLife.17536.019)

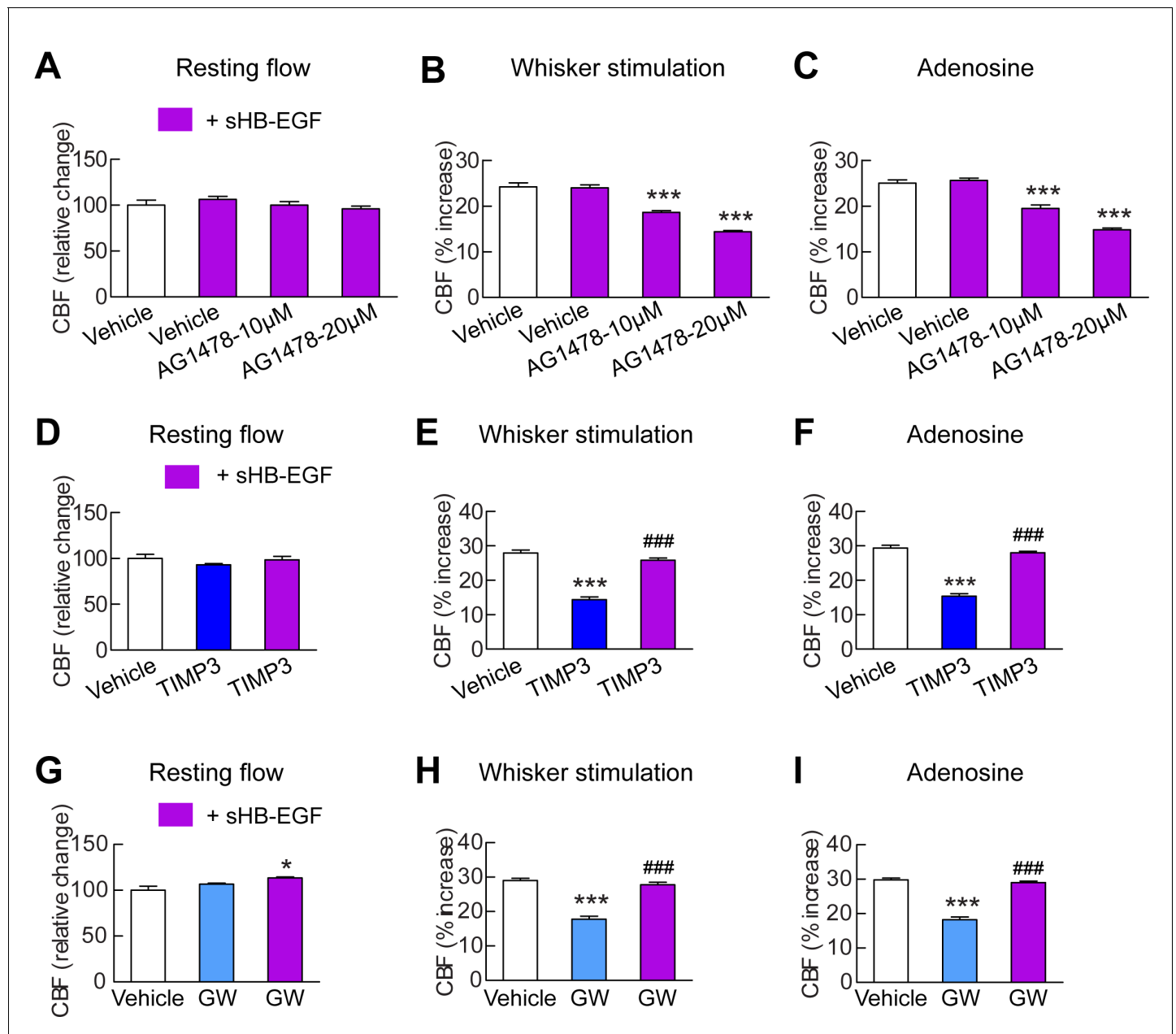


Figure 4. sHB-EGF overcomes CBF deficits induced by ADAM17 inhibition. Effects of sHB-EGF (20 nM) on resting CBF (A, D, G) and whisker stimulation (B, E, H)- and adenosine (C, F, I)-induced CBF responses were assessed in the presence and absence of the ErbB1/ErbB4 inhibitor AG1478 (10 and 20 μ M) (A–C), TIMP3 (40 nM) (D–F) or the ADAM10/ADAM17 inhibitor GW413333X (GW; 5 μ M) (G–I) using a cranial window model. Significance was determined by repeated measure ANOVA followed by Tukey's post-hoc test (* p <0.05, *** p <0.001 compared to vehicle; ### p <0.001 TIMP3+sHB-EGF versus TIMP3 and GW+sHB-EGF versus GW; n = 5/group). Error bars indicate SEM.

DOI: [10.7554/eLife.17536.020](https://doi.org/10.7554/eLife.17536.020)

The following source data is available for figure 4:

Source data 1. Reagents used for **Figure 4**.

DOI: [10.7554/eLife.17536.021](https://doi.org/10.7554/eLife.17536.021)

Source data 2. Main physiological variables of mice studied in **Figure 4**.

DOI: [10.7554/eLife.17536.022](https://doi.org/10.7554/eLife.17536.022)

Source data 3. Numerical data that were used to generate the bar charts in **Figure 4**.

DOI: [10.7554/eLife.17536.023](https://doi.org/10.7554/eLife.17536.023)

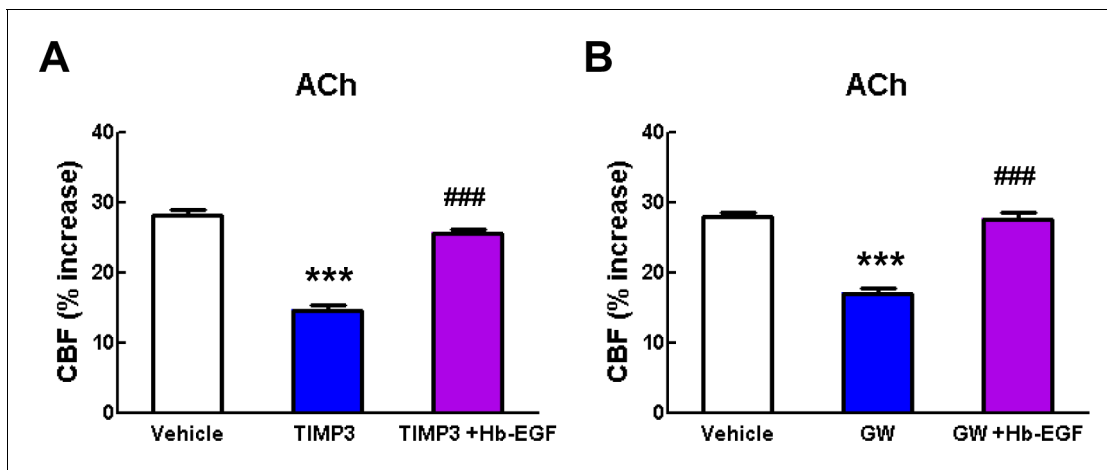


Figure 4—figure supplement 1. Acetylcholine-induced CBF responses impaired by ADAM17 inhibition are ameliorated by exogenous sHB-EGF. (A, B) Effects of sHB-EGF (20 nM) on acetylcholine-induced CBF responses were assessed in the presence and absence of TIMP3 (40 nM) (A) or the ADAM10/ADAM17 inhibitor GW413333X (GW; 5 μM) (B). *** $p < 0.001$ compared to vehicle; ### $p < 0.001$ compared to vehicle. DOI: [10.7554/eLife.17536.024](https://doi.org/10.7554/eLife.17536.024)

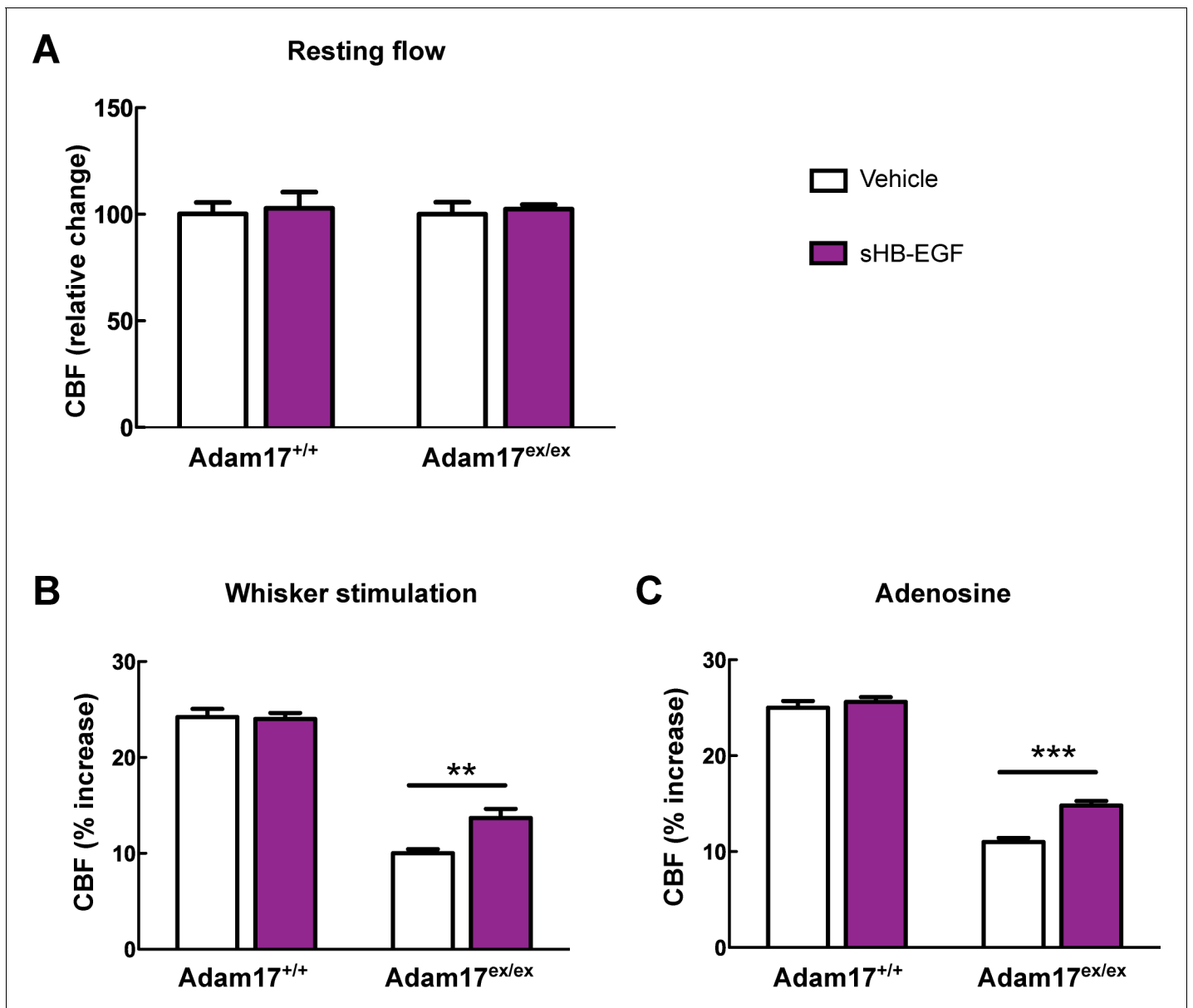


Figure 4—figure supplement 2. CBF deficits induced by ADAM17 deficiency are improved by sHB-EGF. Effects of sHB-EGF (20 nM) on resting CBF (A) and whisker stimulation (B) and adenosine (C)-induced CBF responses were assessed in Adam17^{ex/ex} and wildtype littermate (Adam17^{+/+}) mice. Significance was determined by repeated measure ANOVA followed by Bonferroni post-hoc test (**p < 0.01, ***p < 0.001; n = 5/group).

DOI: [10.7554/eLife.17536.025](https://doi.org/10.7554/eLife.17536.025)

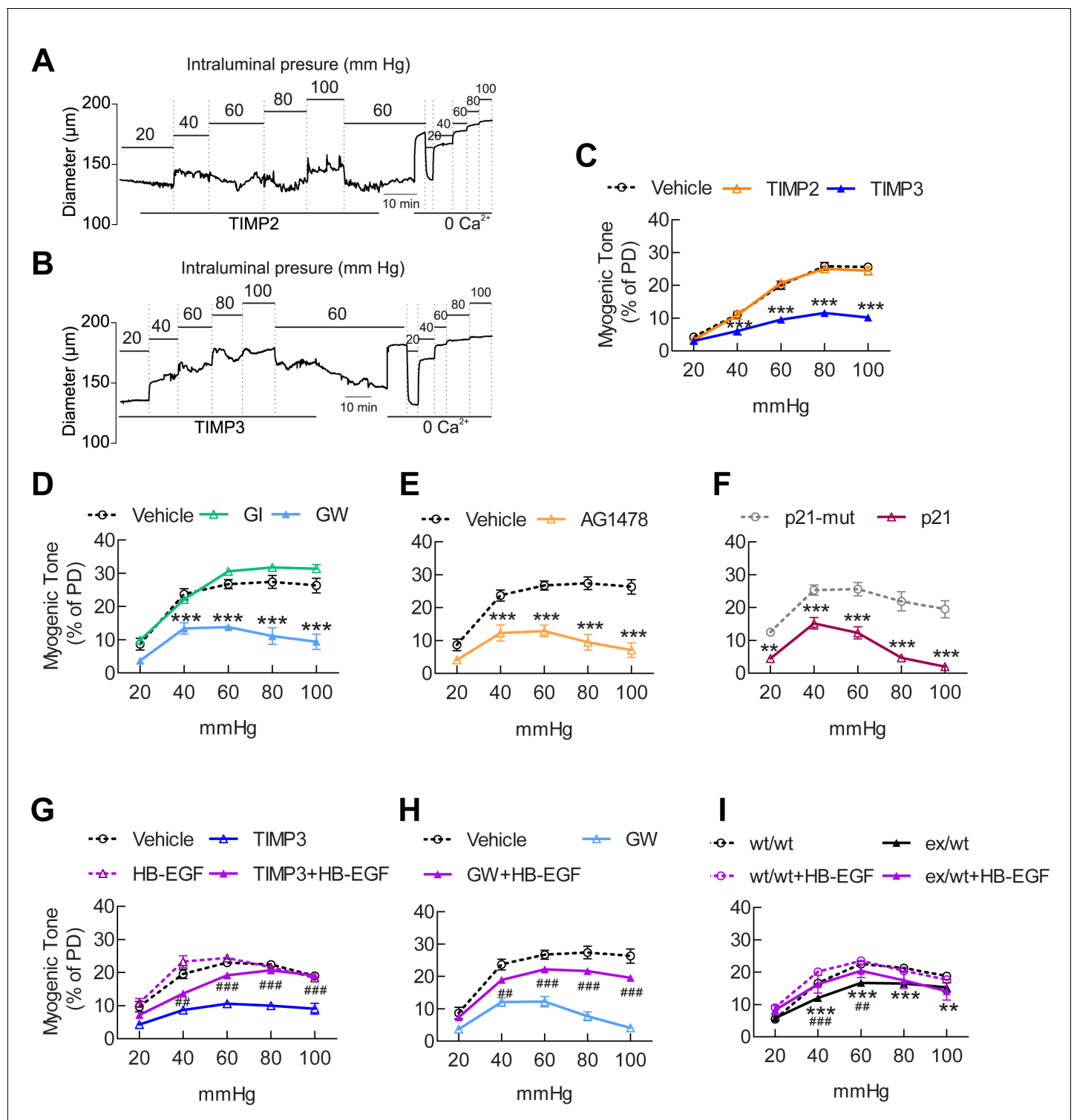


Figure 5. The ADAM17/HB-EGF/(ErbB1/ErbB4) signaling module is involved in regulating the myogenic tone of cerebral arteries. (A–C) Effects of TIMP proteins on the myogenic responses of posterior cerebral arteries to increasing intraluminal pressure. (A, B) Representative internal diameter recordings in the presence of TIMP2 (10 nM) (A) or TIMP3 (8 nM) (B). (C) Summary data of results in (A) and (B). (D–F) Myogenic tone of posterior cerebral arteries, tested in the presence and absence of the dual ADAM10/ADAM17 inhibitor GW41333X (GW; 1 μM), the ADAM10 inhibitor GI254023X (GI; 1 μM) (D), the ErbB1/ErbB4 inhibitor AG1478 (2 μM) (E), the p21 peptide (2.4 μM), and the mutated inactive peptide p21-mut (2.4 μM) (F). (C–F) $^{**}p < 0.01$, $^{***}p < 0.001$ versus vehicle. (G, H) Effects of TIMP3 (8 nM) (g) or GW (1 μM) (H) on the myogenic tone of posterior cerebral arteries were tested in the presence of soluble HB-EGF (3 nM) or vehicle. $^{##}p < 0.01$, $^{###}p < 0.001$, TIMP3+HB-EGF versus TIMP3 and GW+HB-EGF versus GW. (I) Myogenic tone of Figure 5 continued on next page

Figure 5 continued

posterior cerebral arteries was tested in heterozygous *Adam17^{ex/+}* (ex/wt) and *Adam17^{+/+}* (wt/wt) mice in the presence and absence of soluble HB-EGF (3 nM). **p<0.01, ***p<0.001 *Adam17^{ex/+}* versus *Adam17^{+/+}*; ##p<0.01, ###p<0.001, *Adam17^{ex/+}*/HB-EGF versus *Adam17^{ex/+}*). Significance was determined by two-way repeated measures ANOVA followed by Bonferroni post-hoc test (n = 6–8 arteries/group). Error bars indicate SEM.

DOI: [10.7554/eLife.17536.026](https://doi.org/10.7554/eLife.17536.026)

The following source data is available for figure 5:

Source data 1. Reagents used for **Figure 5**.

DOI: [10.7554/eLife.17536.027](https://doi.org/10.7554/eLife.17536.027)

Source data 2. Numerical data that were used to generate the graphs in **Figure 5**.

DOI: [10.7554/eLife.17536.028](https://doi.org/10.7554/eLife.17536.028)

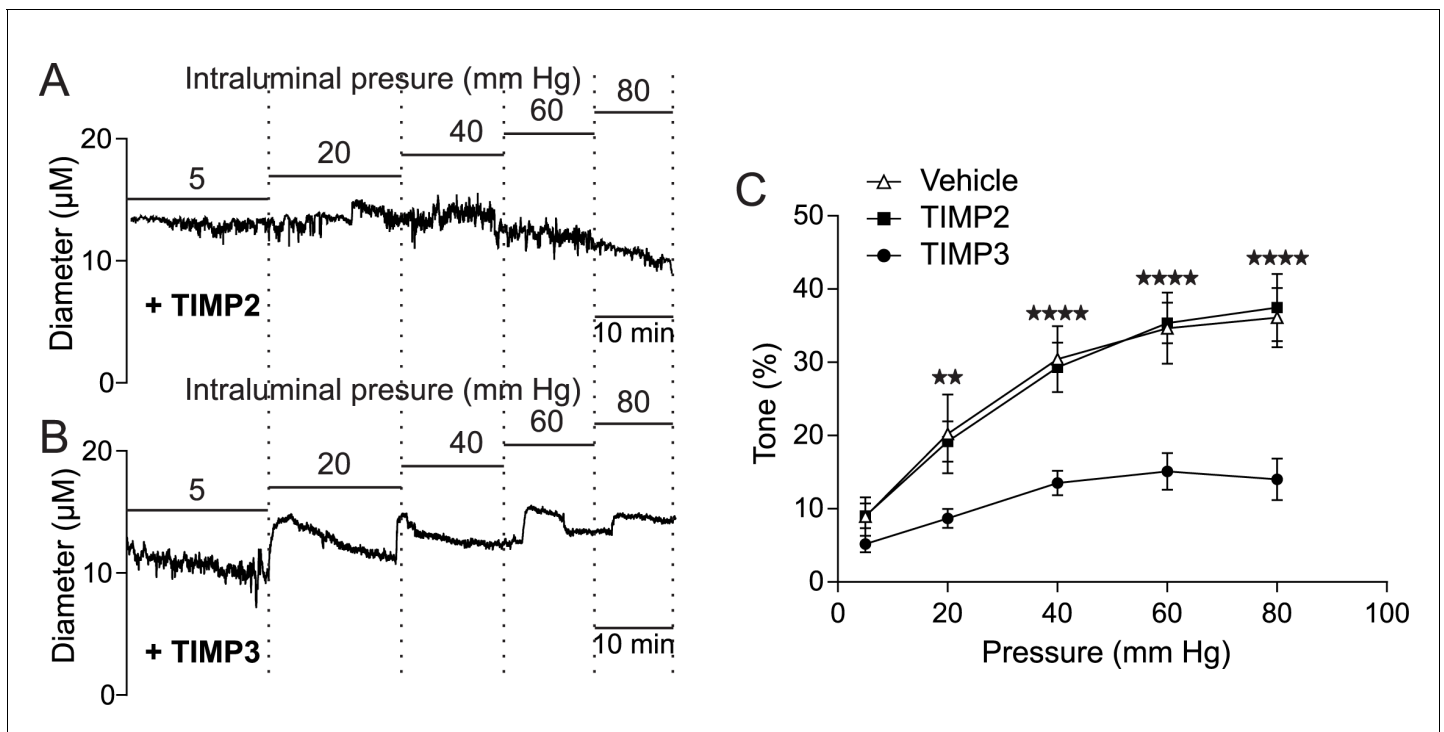


Figure 5—figure supplement 1. TIMP3 strongly impairs myogenic tone of parenchymal arterioles. (A–C) Effects of TIMP proteins on the myogenic responses of parenchymal arterioles to increasing intraluminal pressure. (A, B) Representative internal diameter recordings in the presence of TIMP2 (10 nM) (A) or TIMP3 (8 nM) (B). (C) Summary data of results in (A) and (B). Significance was determined by two-way repeated measures ANOVA followed by Bonferroni post-hoc test. (** $p < 0.01$, **** $p < 0.0001$ $n = 8$ arterioles/group).

DOI: [10.7554/eLife.17536.029](https://doi.org/10.7554/eLife.17536.029)

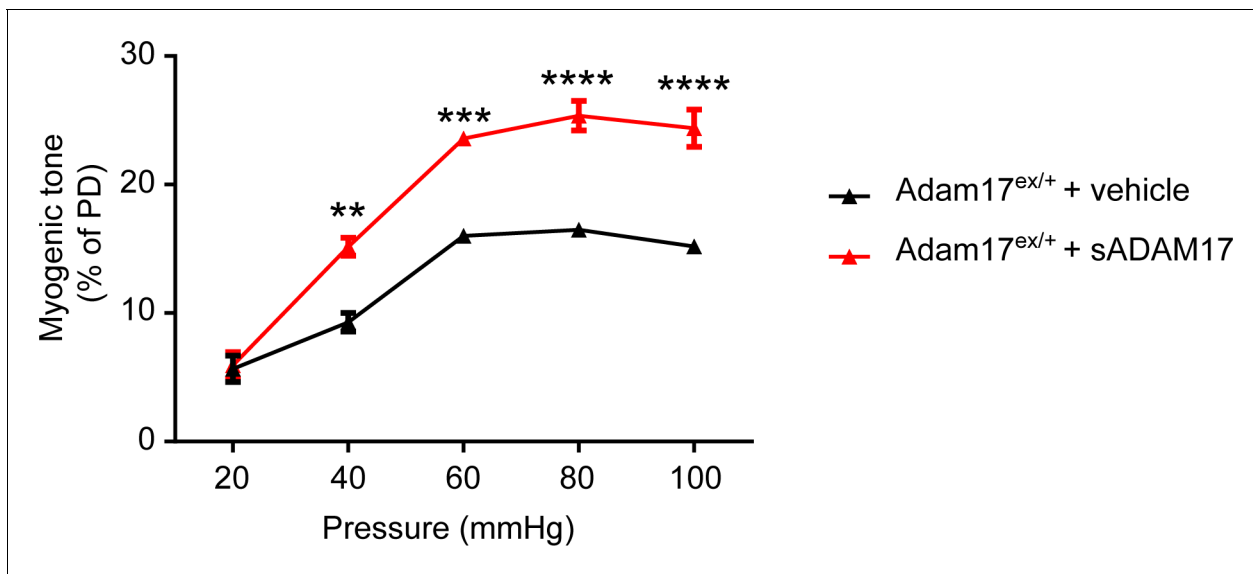


Figure 5—figure supplement 2. sADAM17 ameliorates arterial tone in *Adam17^{ex/+}* mice. Myogenic tone of posterior cerebral arteries was tested in heterozygous *Adam17^{ex/+}* in the presence and absence of soluble ADAM17 (3.2 nM). Significance was determined by two-way repeated measures ANOVA followed by Bonferroni post-hoc test (**p < 0.01, ***p < 0.001, ****p < 0.0001. n = 5–6 arteries/group).

DOI: [10.7554/eLife.17536.030](https://doi.org/10.7554/eLife.17536.030)

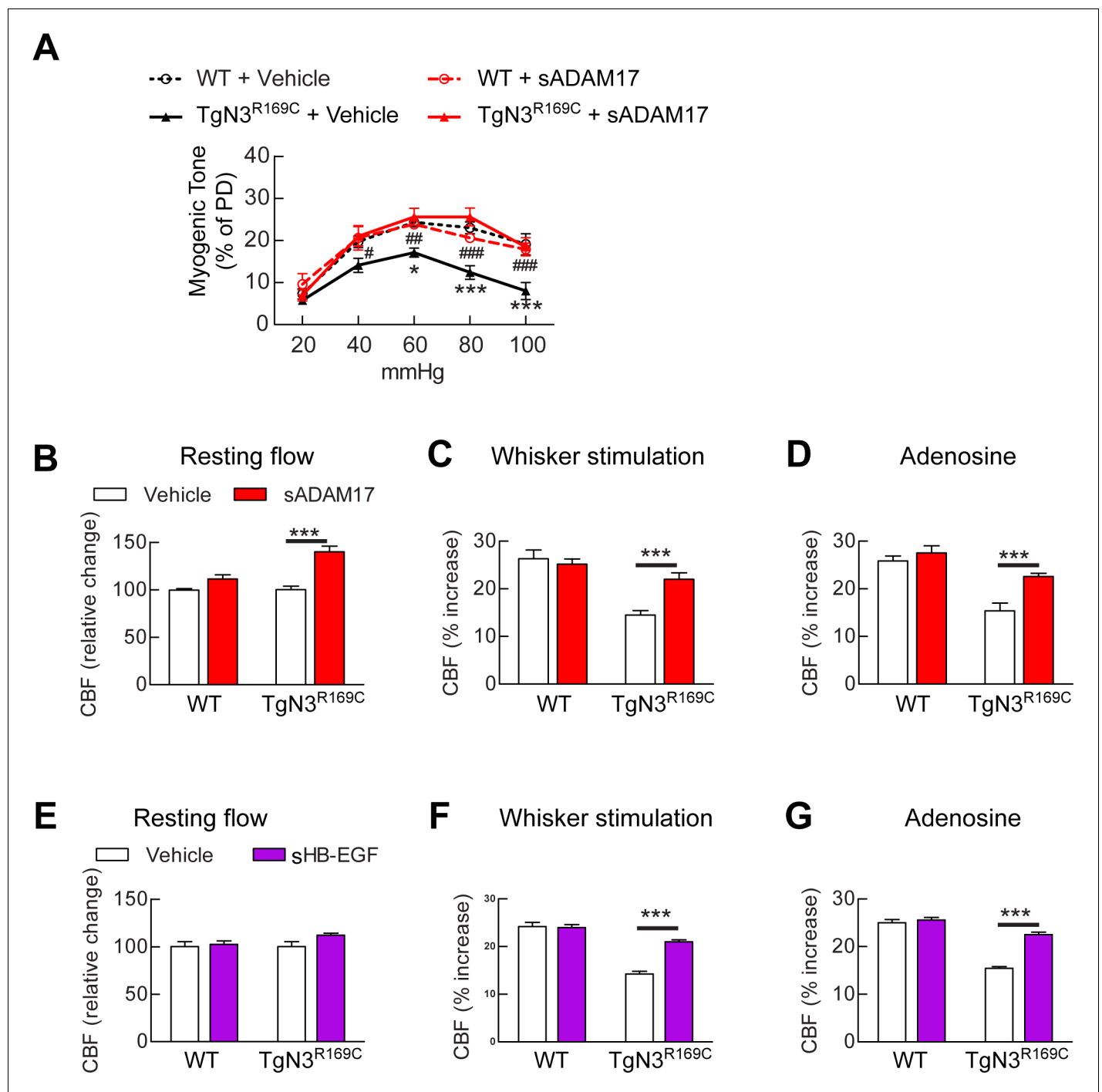


Figure 6. Exogenous sADAM17 and sHB-EGF ameliorate CBF deficits and arterial tone in *TgNotch3^{R169C}* mice. (A) Myogenic tone of posterior cerebral arteries from *TgNotch3^{R169C}* mice (TgN3^{R169C}) and non-transgenic littermates (WT) was tested in the presence of soluble ADAM17 or vehicle. **p*<0.05, ***p*<0.01, ****p*<0.001 versus WT+vehicle; #*p*<0.05, ##*p*<0.01, ###*p*<0.001 TgN3^{R169C}+vehicle versus TgN3^{R169C}+sADAM17 (*n* = 5–7 arteries/ group; 1 artery/mouse). (B–D) Resting CBF (B) and CBF responses to whisker stimulation (C) or adenosine (D) were tested in TgN3^{R169C} and WT mice, before and after superfusion of soluble ADAM17. (E–G) Effects of soluble HB-EGF tested in a second batch of TgN3^{R169C} and WT mice. Significance was determined by two-way repeated measures ANOVA followed by Bonferroni post-hoc test (*n* = 5–6 mice/group). Error bars indicate SEM.

DOI: [10.7554/eLife.17536.031](https://doi.org/10.7554/eLife.17536.031)

The following source data is available for figure 6:

Source data 1. Main physiological variables of mice studied in **Figure 6**.

DOI: [10.7554/eLife.17536.032](https://doi.org/10.7554/eLife.17536.032)

Figure 6 continued on next page

Figure 6 continued

Source data 2. Numerical data that were used to generate the graphs and bar charts in **Figure 6**.

DOI: [10.7554/eLife.17536.033](https://doi.org/10.7554/eLife.17536.033)

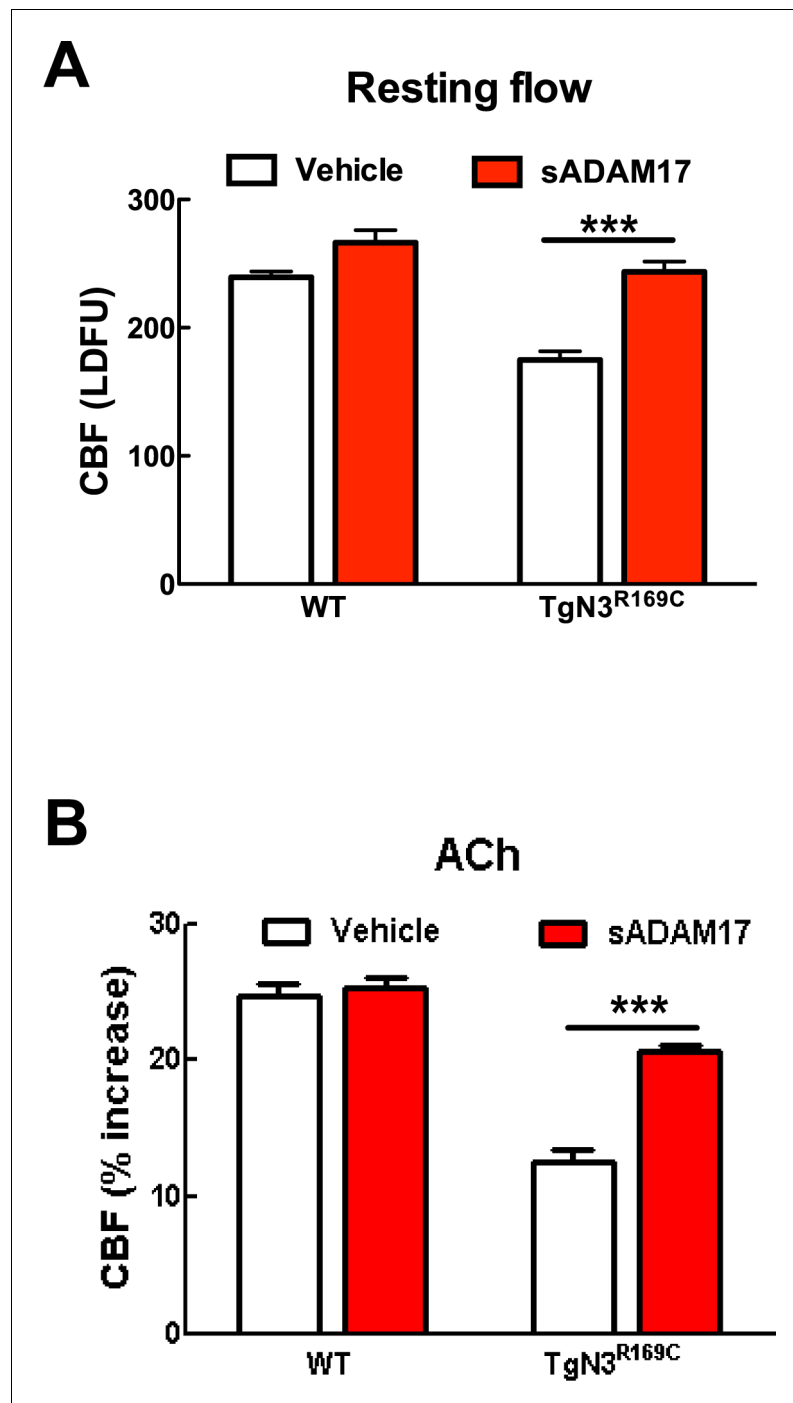


Figure 6—figure supplement 1. Resting CBF and acetylcholine-induced CBF responses impaired by the R169C Notch3 mutation are ameliorated by exogenous sADAM17. Resting CBF, expressed as Laser Doppler flow arbitrary units (LDFU) (A) and CBF responses to acetylcholine (B) were tested in TgNotch3^{R169C} mice (TgN3^{R169C}) and non-transgenic littermates (WT) before and after superfusion of sADAM17 (16 nM). ***p < 0.001. Significance was determined by two-way repeated measures ANOVA followed by Bonferroni post-hoc test (n = 5–6 mice/group).

DOI: [10.7554/eLife.17536.034](https://doi.org/10.7554/eLife.17536.034)

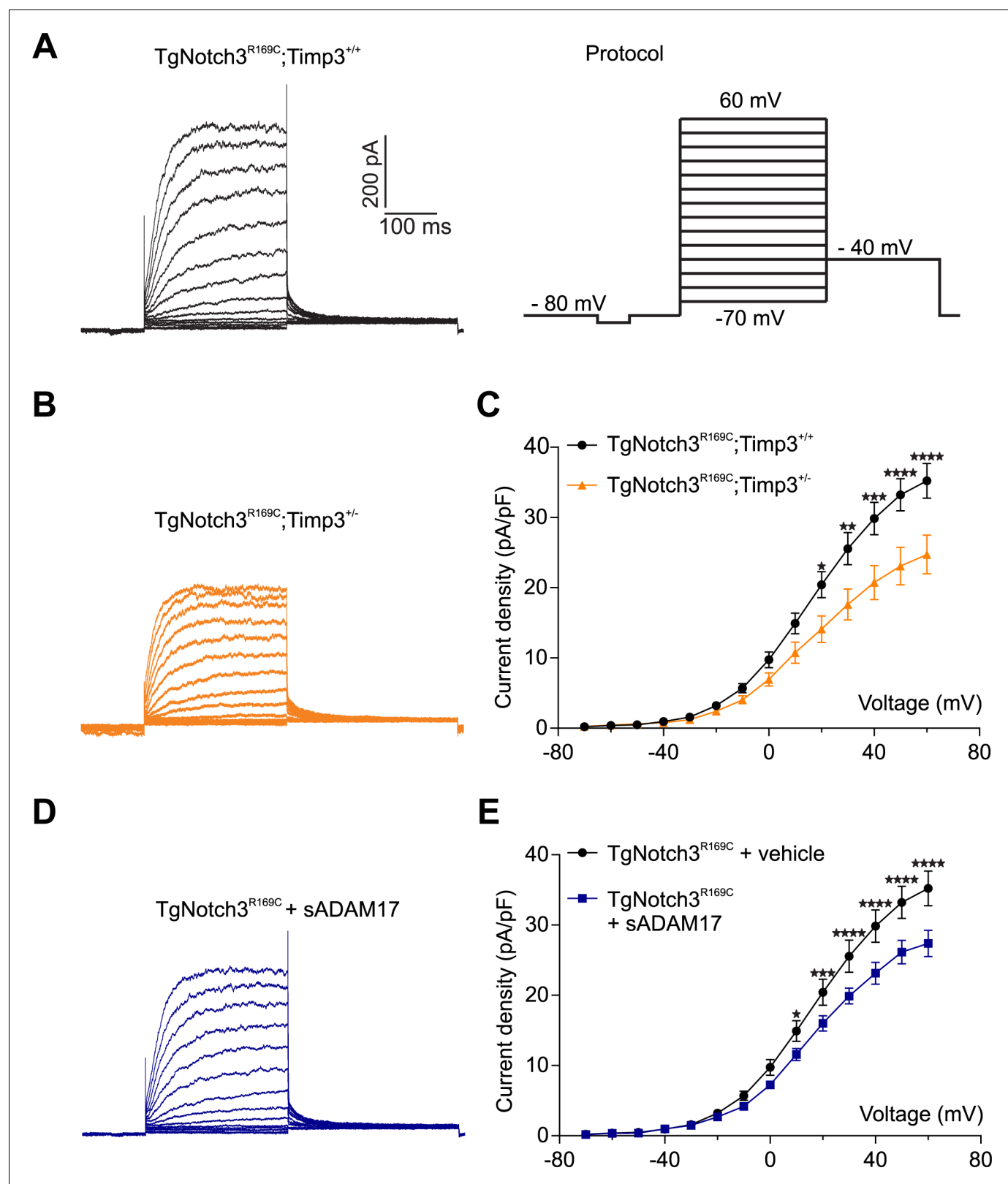


Figure 7. TIMP3 haploinsufficiency and exogenous sADAM17 decrease K_V channel current density in cerebral smooth muscle cells from *TgNotch3*^{R169C} mice. (A,B) Typical family of K_V currents recorded in isolated cerebral smooth muscle cells from double-mutant *TgNotch3*^{R169C}; *Timp3*^{+/-} mice, with *Timp3* haploinsufficiency in the context of *Notch3*^{R169C} overexpression (B), and *TgNotch3*^{R169C}; *Timp3*^{+/+} mice, with wild-type *Timp3* in the context of *Notch3*^{R169C} overexpression (A). (C) Current-voltage (I-V) relationship of K_V currents in cerebral smooth muscle cells from *TgNotch3*^{R169C}; *Timp3*^{+/+} (black circles) and *TgNotch3*^{R169C}; *Timp3*^{+/-} (orange triangles) mice. (D) Typical family of K_V currents recorded in isolated cerebral smooth muscle cells from *TgNotch3*^{R169C} mice treated with vehicle (black circles) or sADAM17 (blue squares). (E) Current-voltage (I-V) relationship of K_V currents in cerebral smooth muscle cells from *TgNotch3*^{R169C} mice treated with vehicle (black circles) or sADAM17 (blue squares). Statistical significance is indicated by asterisks: *p < 0.05, **p < 0.01, ***p < 0.001, ****p < 0.0001.

Figure 7 continued

Notch3^{R169C} overexpression (A) elicited by voltage pulses from −70 mV to +60 mV in the presence of 1 μM paxilline (included to block BK channel currents). (C) Summary of current density results, showing that current density is decreased in myocytes of *TgNotch3*^{R169C};*Timp3*^{+/-} mice compared with those of *TgNotch3*^{R169C};*Timp3*^{+/+} mice. (D) Typical family of K_V currents recorded in isolated cerebral smooth muscle cells from *TgNotch3*^{R169C} mice incubated with soluble ADAM17 (3.2 nM). (E) Summary of current density results, showing that the current density of *TgNotch3*^{R169C} mice is decreased in the presence of sADAM17. Significance was analyzed by two-way repeated measures ANOVA followed by Bonferroni post-hoc test (n = 7–8 cells/group; 1 cell/mouse). Error bars indicate SEM.

DOI: [10.7554/eLife.17536.035](https://doi.org/10.7554/eLife.17536.035)

The following source data is available for figure 7:

Source data 1. Comparison of cerebral K_V current properties.

DOI: [10.7554/eLife.17536.036](https://doi.org/10.7554/eLife.17536.036)

Source data 2. Numerical data that were used to generate the graphs in **Figure 7**.

DOI: [10.7554/eLife.17536.037](https://doi.org/10.7554/eLife.17536.037)

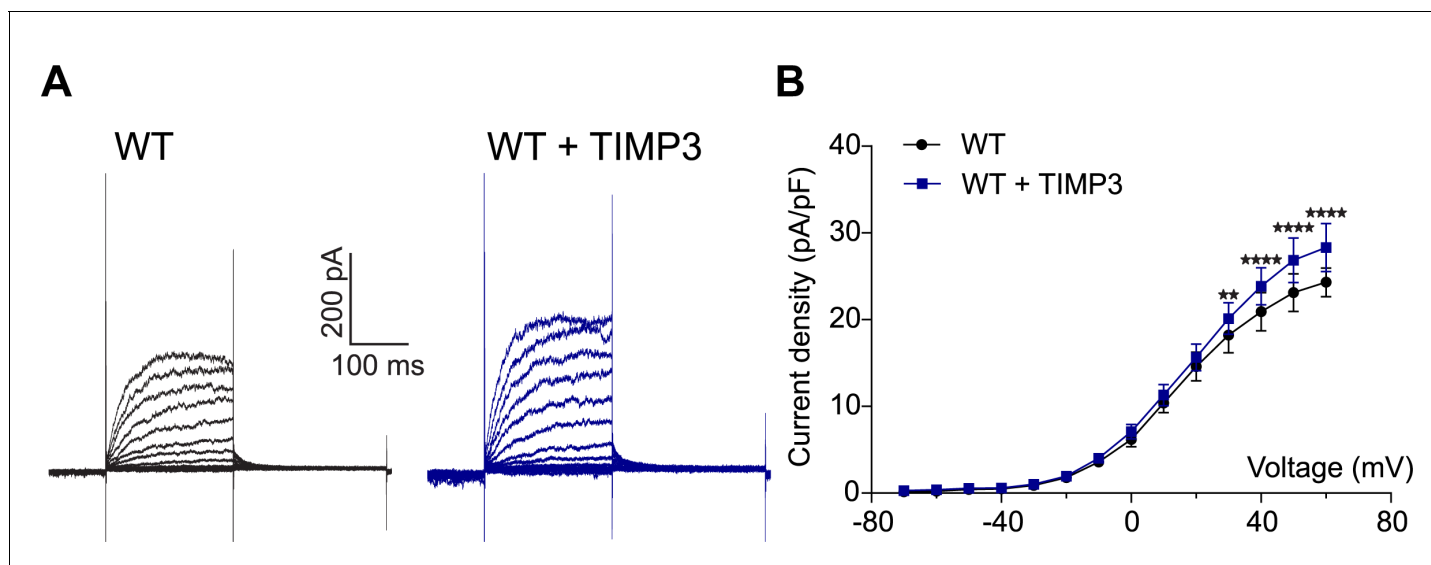


Figure 7—figure supplement 1. Exogenous TIMP3 increases voltage-gated potassium (K_V) channel current density in cerebral smooth muscle cells. (A) Typical family of K_V currents recorded in isolated cerebral smooth muscle cells from non-Tg (WT) mice incubated with TIMP3 (8 nM) or vehicle and elicited by voltage pulses from -70 mV to $+60$ mV in the presence of $1 \mu\text{M}$ paxilline (included to block BK channel currents). (B) Summary of current density results, showing that exogenous TIMP3 increases current density. Significance was analyzed by two-way repeated measures ANOVA followed by Bonferroni post-hoc test ($n = 5$ cells /group; 1 cell/mouse).

DOI: [10.7554/eLife.17536.038](https://doi.org/10.7554/eLife.17536.038)

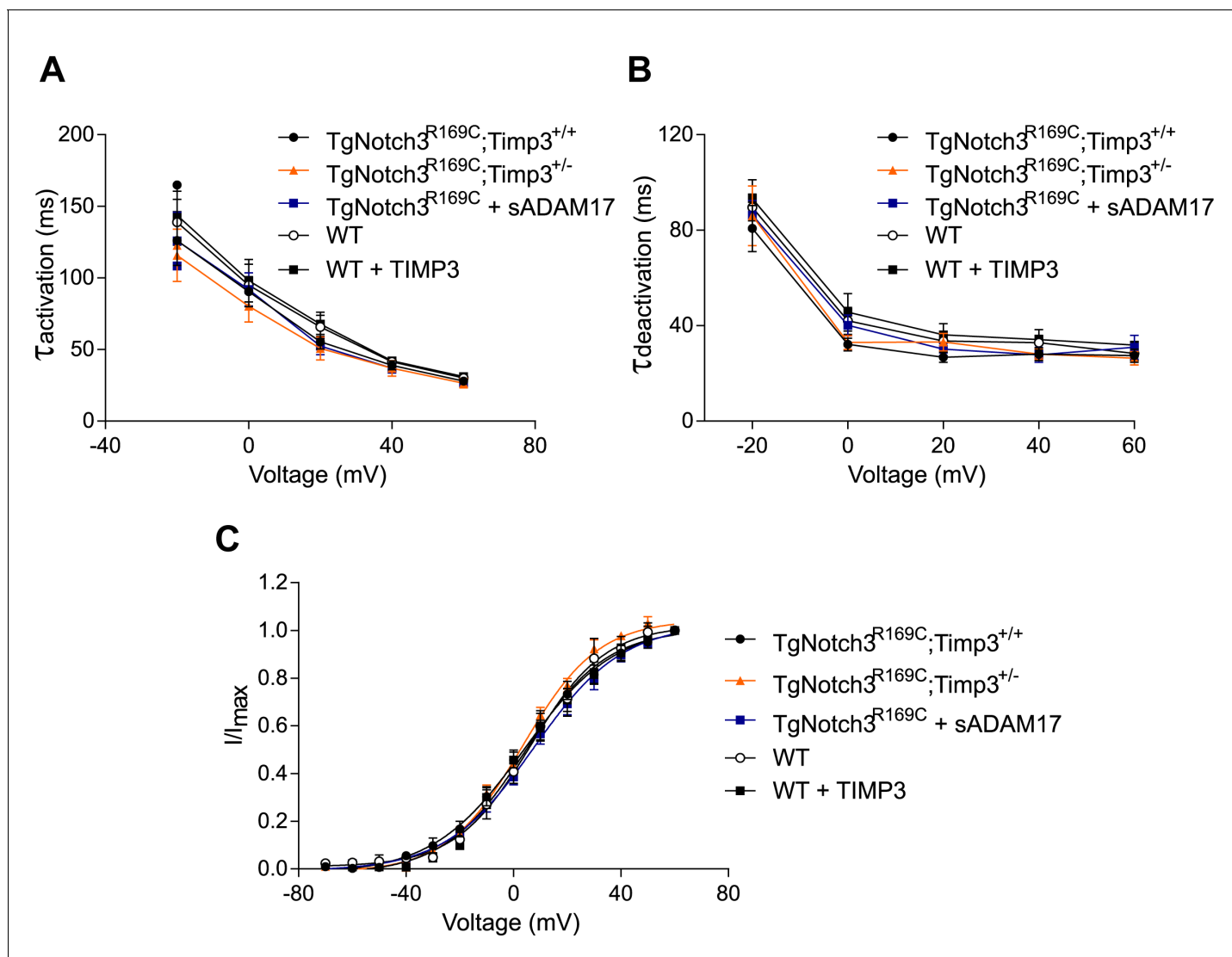


Figure 7—figure supplement 2. Analyses of cerebral K_V current properties. (A) Activation time constants (τ_{activation}) were determined from an exponential fit of individual voltage-evoked current traces. (B) De-activation time constants (τ_{deactivation}), obtained from an exponential fit of tail currents at −40 mV. (C) Steady-state activation properties of K_V currents measured from normalized tail currents. The voltage for half-maximal activation (V_{1/2}) and the factor k were obtained from a fit of the data to the Boltzman equation.

DOI: [10.7554/eLife.17536.039](https://doi.org/10.7554/eLife.17536.039)

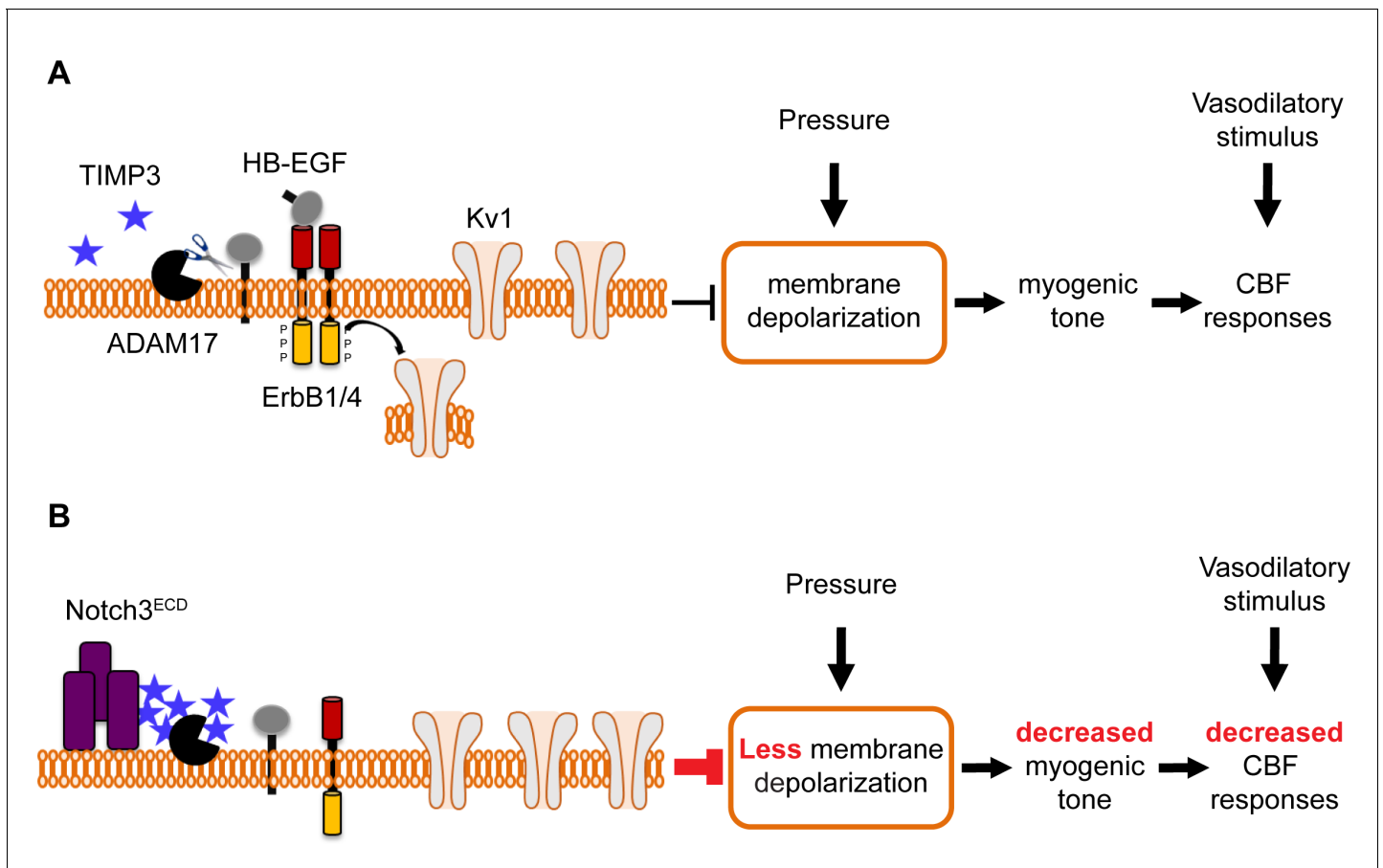


Figure 8. Proposed model of TIMP3 regulation of cerebral arterial tone and CBF responses. **(A)** Under physiological conditions (upper panel), TIMP3 is present in a low abundance in the extracellular matrix of brain arteries. ADAM17 at the cell surface of cerebral arterial myocytes is therefore active and able to cleave and release sHB-EGF, resulting in ErbB1/ErbB4 activation and Kv1 channel endocytosis. The internalization of Kv1 channels relieves the tonic hyperpolarizing influence of these channels on the membrane potential of arterial myocytes, thereby allowing full development of pressure-induced vasoconstriction (myogenic tone) of brain arteries and enabling full CBF responses to whisker stimulation and vasodilators. **(B)** In CADASIL (lower panel), Notch3^{ECD} accumulates at the surface of smooth muscle cells, leading to an increase in the amount of TIMP3, which binds to and inhibits ADAM17, blunting sHB-EGF release and ErbB1/ErbB4 activity, and thereby decreasing Kv1 endocytosis. The resulting increase in Kv1 current density hyperpolarizes arterial myocytes, acting as a brake to limit the development of myogenic tone and evoked CBF responses.

DOI: [10.7554/eLife.17536.040](https://doi.org/10.7554/eLife.17536.040)